

# A Comparative Study of Two New Structure Types. Synthesis and Structural and Electronic Characterization of $K(\text{RE})\text{P}_2\text{Se}_6$ ( $\text{RE} = \text{Y}, \text{La}, \text{Ce}, \text{Pr}, \text{Gd}$ )

John H. Chen,<sup>†</sup> Peter K. Dorhout,<sup>\*,†</sup> and J. E. Ostenson<sup>‡</sup>

Department of Chemistry, Colorado State University, Fort Collins, Colorado 80523, and Ames Laboratory, U.S. Department of Energy, Ames, Iowa 50011

Received December 19, 1995<sup>⊗</sup>

Two polytypes of potassium rare-earth-metal hexaselenodiphosphates(IV),  $K(\text{RE})\text{P}_2\text{Se}_6$  ( $\text{RE} = \text{Y}, \text{La}, \text{Ce}, \text{Pr}, \text{Gd}$ ), have been synthesized from the stoichiometric reaction of RE, P, Se, and  $\text{K}_2\text{Se}_4$  at 750 °C. Both single-crystal and powder X-ray diffraction analyses showed that the structures of these polytypes vary with the size of the rare earth metals. For the smaller rare-earth metals, Y and Gd,  $K(\text{RE})\text{P}_2\text{Se}_6$  crystallized in the orthorhombic space group  $P2_12_12_1$ . The yttrium compound was studied by single-crystal X-ray diffraction with the cell parameters  $a = 6.7366(5)$  Å,  $b = 7.4286(6)$  Å,  $c = 21.603(2)$  Å, and  $Z = 4$ . This structure type comprises a layered, square network of yttrium atoms that are bound to four distinct  $[\text{P}_2\text{Se}_6]^{4-}$  units through selenium bonding. Each  $[\text{P}_2\text{Se}_6]^{4-}$  unit possesses a Se atom that is not bound to any Y atom but is pointing out into the interlayer spacing, into an environment of potassium cations. For larger rare-earth metals, La, Ce, and Pr,  $K(\text{RE})\text{P}_2\text{Se}_6$  crystallized in a second, monoclinic polytype, the structure of which has been published. Both of these two different polytypes can be related to each other and several other isoelectronic chalcophosphate structures based on a Parthé valence electron concentration analysis. These structures include  $\text{Ag}_4\text{P}_2\text{S}_6$ ,  $\text{K}_2\text{FeP}_2\text{S}_6$ , and the hexagonal  $\text{M}^{\text{II}}\text{PS}_3$  structure types. The magnetic susceptibilities of the title compounds have been studied, and the behavior can be explained based on a simple set of unpaired f-electrons. The diffuse reflectance spectroscopy also showed that these yellow plates are moderately wide band gap ( $\sim 2.75$  eV) semiconductors.

## Introduction

We recently reported the synthesis and structure of the first lanthanide selenodiphosphate (IV),  $\text{KLaP}_2\text{Se}_6$ .<sup>1</sup> This structure prompted us to examine the effects of lanthanide size on the structure as well as to examine the magnetic and electronic characteristics of these new materials. Since this newly reported phase is isoelectronic to  $\text{Ag}_4\text{P}_2\text{S}_6$ ,  $\text{K}_2\text{FeP}_2\text{S}_6$ , and the family of  $\text{M}^{\text{II}}\text{P}_2\text{Q}_6$  layered structures,<sup>2–7</sup> we have also tried to find a correlation between these structures and our new lanthanide selenodiphosphates(IV).

The interest in these compounds was prompted by the relationship seen between the “oxo” phosphates and the “chalco” phosphates that has been recently described. Examples include the following: from Brockner,  $\text{Pb}_2\text{P}_2\text{Se}_6$ ,<sup>8</sup>  $\text{PrPS}_4$ ,<sup>9</sup>  $\text{K}_2\text{Mn}(\text{Fe})\text{P}_2\text{S}_6$ ,<sup>6,7</sup>  $\text{CuHgPS}_4$ ,<sup>10</sup>  $\text{TlSnPS}_4$ ,<sup>11</sup>  $\text{Hg}_2\text{P}_2\text{Se}_6$ ,<sup>12</sup>  $\text{Ti}_4\text{P}_2\text{Se}_6$ ,<sup>13</sup> and

$\text{Eu}_2\text{P}_2\text{S}_6$ , the first rare-earth thiodiphosphate;<sup>14a</sup> from Kanatzidis,  $\text{KMP}_2\text{Se}_6$  (Sb, Bi),<sup>15</sup>  $\text{Cs}_8\text{M}_4(\text{P}_2\text{Se}_6)_5$  (Sb, Bi),<sup>16</sup>  $\text{ABiP}_2\text{S}_7$  (K, Rb),<sup>17</sup>  $\text{A}_2\text{MP}_2\text{Se}_6$  (Mn, Fe),  $\text{A}_2\text{M}_2\text{P}_2\text{Se}_6$  (Cu, Ag),<sup>18</sup>  $\text{A}_4\text{Ti}_2\text{P}_6\text{Se}_{25}$ ,  $\text{ATiPSe}_5$ ,<sup>19</sup>  $\text{A}_4\text{Pb}(\text{PSe}_4)_2$  and  $\text{K}_4\text{Eu}(\text{PSe}_4)_2$ ,<sup>20</sup> from Kolis,  $(\text{Ph}_4\text{P})_2[\text{Se}=\text{W}(\text{PSe}_4)(\text{PSe}_2)]^{21}$  and  $(\text{Ph}_4\text{P})_2[\text{P}_2\text{Se}_8]$ ;<sup>22</sup> from Tremel,  $\text{K}_4\text{Ti}_2\text{P}_6\text{S}_{25}$ ,  $\text{KVP}_2\text{S}_7$ ,  $\text{K}_3\text{V}_2\text{P}_3\text{S}_{12}$ ,  $\text{K}_3\text{Ti}_2\text{P}_5\text{S}_{18}$ , and  $\text{K}_2\text{VP}_2\text{S}_7$ ;<sup>23</sup> and from our own work,  $\text{K}_3\text{Cu}_3\text{P}_3\text{Se}_9$ .<sup>24</sup> We believed that there should also exist a family of lanthanide chalcophosphates that may be related to the family of lanthanide oxophosphates (1-dimensional tunnel structures).<sup>25–27</sup> Indeed, these new compounds may display unique electronic or magnetic properties resulting from the more covalent nature of the heavier chalcogenides. This paper describes the detailed study of a series of rare-earth selenodiphosphate(IV) compounds,  $K(\text{RE})\text{P}_2\text{Se}_6$  (RE

\* Author to whom correspondence should be addressed. Fax: 970-491-1801. E-mail: PKD@LAMAR.COLOSTATE.EDU.

<sup>†</sup> Colorado State University.

<sup>‡</sup> U.S. Department of Energy.

<sup>⊗</sup> Abstract published in *Advance ACS Abstracts*, August 15, 1996.

- (1) Chen, J. H.; Dorhout, P. K. *Inorg. Chem.* **1995**, *34*, 5705.
- (2) Klingen, W.; Eulenberger, G.; Hahn, H. *Naturwissenschaften* **1968**, *55*, 229.
- (3) Klingen, W.; Eulenberger, G.; Hahn, H. *Naturwissenschaften* **1970**, *57*, 88.
- (4) Klingen, W.; Ott, R.; Hahn, H. *Z. Anorg. Allg. Chem.* **1973**, *396*, 271.
- (5) Toffoli, P.; Michelet, A.; Khodadad, P.; Rodier, N. *Acta Crystallogr. B* **1982**, *38*, 706.
- (6) Carrillo-Cabrera, W.; Sassmannshausen, J.; von Schnering, H. G.; Menzel, F.; Brockner, W. *Z. Anorg. Allg. Chem.* **1994**, *620*, 489.
- (7) Menzel, F.; Brockner, W.; Carrillo-Cabrera, W.; von Schnering, H. G. *Z. Anorg. Allg. Chem.* **1994**, *620*, 1081.
- (8) Becker, R.; Brockner, W.; Schäfer, H. *Z. Naturforsch.* **1984**, *39A*, 357.
- (9) Wibbelmann, C.; Brockner, W.; Eisenmann, B.; Schäfer, H. *Z. Naturforsch.* **1984**, *A39*, 190.
- (10) Menzel, F.; Brockner, W.; Carrillo-Cabrera, W. *Heteroatom. Chem.* **1993**, *4*, 393.
- (11) Becker, R.; Brockner, W.; Eisenmann, B. *Z. Naturforsch.* **1987**, *A42*, 1309.
- (12) Brockner, W.; Paetzmann, U. *Z. Naturforsch.* **1987**, *42A*, 517.
- (13) Brockner, W.; Ohse, L.; Paetzmann, U.; Eisenmann, B.; Schäfer, H. *Z. Naturforsch.* **1985**, *A40*, 1248.
- (14) (a) Brockner, W.; Becker, R. *Z. Naturforsch.* **1987**, *A42*, 511. (b)  $\text{Eu}_2\text{P}_2\text{Se}_6$  crystallizes in  $P2_1/n$ , with  $a = 6.913(1)$  Å,  $b = 7.761(2)$  Å,  $c = 9.769(2)$  Å, and  $\beta = 91.51(2)^\circ$ . A crystal structure and magnetic study of this compound are forthcoming.
- (15) McCarthy, T. J.; Kanatzidis, M. G. *J. Chem. Soc., Chem. Commun.* **1994**, 1089.
- (16) McCarthy, T. J.; Hogan, T.; Kannewurf, C. R.; Kanatzidis, M. G. *Chem. Mater.* **1994**, *6*, 1072.
- (17) McCarthy, T. J.; Kanatzidis, M. G. *Chem. Mater.* **1993**, *5*, 1061.
- (18) McCarthy, T. J.; Kanatzidis, M. G. *Inorg. Chem.* **1995**, *34*, 1257.
- (19) Chondroudis, K.; Kanatzidis, M. G. *Inorg. Chem.* **1995**, *34*, 5401.
- (20) Chondroudis, K.; McCarthy, T. J.; Kanatzidis, M. G. *Inorg. Chem.* **1996**, *35*, 840.
- (21) O'Neal, S. C.; Pennington, W. T.; Kolis, J. W., *Angew. Chem., Int. Ed. Engl.* **1990**, *29*, 1486.
- (22) Zhao, J.; Pennington, W. T.; Kolis, J. W. *J. Chem. Soc., Chem. Commun.* **1992**, 265.
- (23) Tremel, W.; Kleinke, H.; Derstroff, V.; Reisner, C. *J. Alloys Compd.* **1995**, *219*, 73.
- (24) Dorhout, P. K.; Malo, T. M. *Z. Anorg. Allg. Chem.* **1996**, *622*, 385.
- (25) Mooney, R. C. L. *J. Chem. Phys.* **1948**, *16*, 1003.
- (26) Mooney, R. C. L. *Acta Crystallogr.* **1950**, *3*, 337.
- (27) Beall, G. W.; Boatner, L. A.; Mullica, D. F.; Milligan, W. O. *J. Inorg. Nucl. Chem.* **1981**, *43*, 101.

**Table 1.** Crystal Data Parameters for  $\text{KYP}_2\text{Se}_6$ 

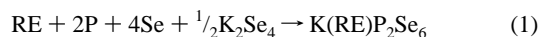
space group (No.), $Z$	$P2_12_12_1$ (19), 4	calcd density ( $\text{g}/\text{cm}^3$ )	4.078
$a$ ( $\text{\AA}$ )	6.7366(5)	$\mu$ ( $\text{mm}^{-1}$ )	26.207
$b$ ( $\text{\AA}$ )	7.4286(6)	radiation (Mo $K\alpha$ ) ( $\text{\AA}$ )	0.710 73
$c$ ( $\text{\AA}$ )	21.603(2)	temp ( $^\circ\text{C}$ )	23
$V$ ( $\text{\AA}^3$ )	1081.1(2)	$R$ (%) <sup>a</sup>	4.02
fw	663.71	wR2 (%) <sup>b</sup>	8.37 <sup>c</sup>

<sup>a</sup>  $R = \sum ||F_o| - |F_c|| / \sum |F_o|$ . <sup>b</sup>  $wR2 = [\sum w(F_o^2 - F_c^2)^2 / \sum w(F_o^2)]^{1/2}$ . <sup>c</sup>  $w^{-1} = [\sigma^2(F_o^2) + (0.0410P)^2]$  where  $P = (F_o^2 + F_c^2)/3$ .

= Y, La, Ce, Pr, Gd) that can be found in either our previously described structure<sup>1</sup> or in a new, single layered polytype,  $\text{KYP}_2\text{Se}_6$ , as well as the magnetic and electronic behavior of this new family of compounds.

### Experimental Section

The general procedure for the preparation of  $\text{K(RE)}\text{P}_2\text{Se}_6$  (RE = Y, La, Ce, Pr, Gd) is as follows: The title compounds were prepared by reacting the rare-earth metal (99.999%, Ames lab), elemental phosphorus (99.999%, Johnson Matthey), selenium metal (99.999%, Johnson Matthey), and  $\text{K}_2\text{Se}_4$  (prepared from stoichiometric amounts of K and Se in liquid ammonia<sup>28</sup>) together, according to (1). In the original



synthesis of  $\text{KLaP}_2\text{Se}_6$ , the ratio of Se to  $\text{K}_2\text{Se}_4$  was 10:1, and the flux was in 200% excess for the reaction.<sup>1</sup> We have discovered that the excess flux is not necessary for crystal growth at higher temperatures, and the reactions tend to be much cleaner. Thus far, we have prepared the two polytypic phases with Y, La, Ce, Pr, and Gd. Reactions with europium yielded a phase that is isostructural with  $\text{Eu}_2\text{P}_2\text{S}_6$ ,<sup>14</sup> and the magnetic and spectroscopic properties of this material will be discussed elsewhere.

The reactants (typical reaction scale is 0.10 mmol rare-earth metal) were loaded in a nitrogen atmosphere glove box and sealed under vacuum in fused silica ampoules. The ampoules were then heated in a furnace to 750  $^\circ\text{C}$  (50  $^\circ\text{C}/\text{h}$ ) for 100 hours, and cooled to ambient temperature at 5  $^\circ\text{C}/\text{h}$  to yield X-ray quality single crystals. Nearly quantitative yields of single-phase powders could be obtained at temperatures as low as 350  $^\circ\text{C}$ . The products were then quickly washed with distilled water to remove unreacted  $\text{K}_2\text{Se}_4$ . The products are mildly moisture sensitive but no significant loss of product was noticed upon washing with water. The  $\text{K(RE)}\text{P}_2\text{Se}_6$  stoichiometry was verified by EDS. Yields: generally > 80% based on rare-earth metal (from X-ray diffraction).

**Syntheses:**  $\text{KYP}_2\text{Se}_6$ , 8.9 mg of Y (0.10 mmol), 6.2 mg of P (0.20 mmol), 31.6 mg of Se (0.40 mmol), and 19.7 mg of  $\text{K}_2\text{Se}_4$  (0.5 mmol);  $\text{KLaP}_2\text{Se}_6$ , 13.9 mg of La (0.10 mmol), 6.2 mg of P (0.20 mmol), 31.6 mg of Se (0.40 mmol), and 19.7 mg of  $\text{K}_2\text{Se}_4$  (0.5 mmol);<sup>1</sup>  $\text{KCeP}_2\text{Se}_6$ , 14.0 mg of Ce (0.10 mmol), 6.2 mg of P (0.20 mmol), 31.6 mg of Se (0.40 mmol), and 19.7 mg of  $\text{K}_2\text{Se}_4$  (0.5 mmol);  $\text{KPrP}_2\text{Se}_6$ , 14.1 mg of Pr (0.10 mmol), 6.2 mg of P (0.20 mmol), 31.6 mg of Se (0.40 mmol), and 19.7 mg of  $\text{K}_2\text{Se}_4$  (0.5 mmol);  $\text{KGdP}_2\text{Se}_6$ , 15.7 mg of Gd (0.10 mmol), 6.2 mg of P (0.20 mmol), 31.6 mg of Se (0.40 mmol), and 19.7 mg of  $\text{K}_2\text{Se}_4$  (0.5 mmol).

**X-ray Structure Determination.** A suitable single crystal (0.36  $\times$  0.16  $\times$  0.09 mm) of  $\text{KYP}_2\text{Se}_6$ , as determined from rotation photographs, was mounted on a Siemens 4-circle P4 diffractometer and analyzed at room temperature. Details of the crystallographic data collection can be found in Table 1. The unit cell was determined from at least 25 centered reflections randomly found between 10 and 25 $^\circ$  in  $2\theta$ . Axial photographs confirmed the axial lengths and Laue class. Graphite-monochromated Mo  $K\alpha$  radiation was used. Data was collected by  $\theta$ - $2\theta$  scans over one quadrant ( $6.0 \leq \theta \leq 64^\circ$ ) for  $+h$ ,  $\pm k$ ,  $\pm l$ , yielding 3518 reflections collected (1514 observed), and a semi-empirical absorption correction, as determined by  $\psi$ -scans (range of transmission, 0.103–0.649), was applied to the data and a secondary extinction coefficient was refined ( $2.0 \times 10^{-4}$ ). The structure was solved by direct methods and all atoms refined anisotropically with

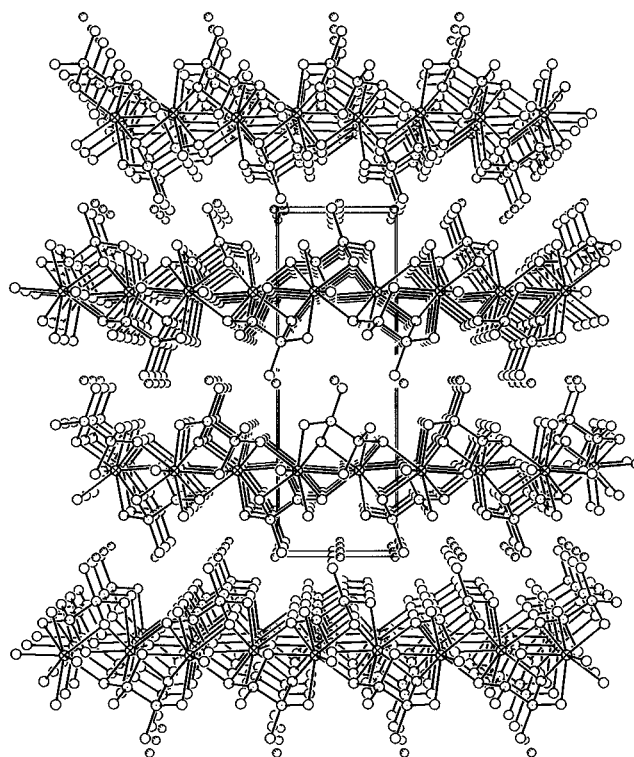


**Figure 1.** View down (100) of  $\text{KYP}_2\text{Se}_6$ . Open circles are Se; dotted circles, P; crossed circles, Y; and shaded circles, K. The unit cell boundaries are shown.

SHELXTL using full-matrix least-squares refinement on  $F^2$  for 93 variables.<sup>29</sup> The correct enantiomorph in  $P2_12_12_1$  could not be verified by the Flack analysis,<sup>30,31</sup> and the structure was subsequently solved as a racemic twin, with the Flack parameter refining to 0.42(3). The largest residuals were +1.12 and  $-1.25 \text{ e}^-/\text{\AA}^3$ . The final goodness of fit was 1.041. The unit cell parameters of all of the compounds in the study were determined from either their single-crystal or powder X-ray diffraction patterns and<sup>32</sup> collected with an Enraf-Nonius 601 generator and Guinier camera and are listed in Table 2.

**Physical Property Measurements.** The variable temperature magnetic data were recorded on a Quantum Design 5 T SQUID magnetometer in a field of 2 T. Samples were loaded into a fused silica tube with a variable fused silica plunger array so as to minimize the inhomogeneity effects of the sample holder. Energy dispersive spectroscopy (EDS) was performed with Philips 505 SEM equipped with a Kevex detector and analysis software. UV/vis/near-IR diffuse reflectance spectra were recorded with a Hitachi U-3501 spectrophotometer equipped with a 60 mm diameter integrating sphere accessory. Samples were mounted on MgO plates. Spectra were transformed into  $\log(\alpha/S)$  vs energy plots in the manner of the Kubelka–Munk relationship.<sup>33</sup>

### Results

**Structure of  $\text{KYP}_2\text{Se}_6$ .** The structure of  $\text{KYP}_2\text{Se}_6$  is illustrated in Figures 1 and 2. The compound comprises a single, square network of yttrium atoms that are contained in an environment of eight selenium atoms, Figure 3. The selenium atoms are each part of four distinct selenodiphosphate(IV) units. Each selenodiphosphate(IV) unit possesses a selenium atom Se(6) that is not bound to any yttrium atoms but is rather

- (29) Sheldrick, G. M. *J. Appl. Crystallogr.*, manuscript in preparation.  
 (30) Flack, H. D. *Acta Crystallogr.*, A **1983**, 39, 876.  
 (31) Bernardinelli, G.; Flack, H. D., *Acta Crystallogr.*, A **1985**, 41, 500.  
 (32) Evain, M. *U-FIT: A cell parameter refinement program*; I.M.N.: Nantes, France, 1992.  
 (33) Wilkinson, F.; Kelly, G. In *CRC Handbook of Organic Photochemistry*; J. C. Scaiano, J. C., Ed.; CRC Press: Boca Raton, FL, 1989; Vol. 1, 293.

**Table 2.** Crystallographic and Magnetic Parameters

compound	space group	<i>a</i> (Å)	<i>b</i> (Å)	<i>c</i> (Å)	$\beta$ (deg)	$\mu_{\text{BM}}$ (Bohr mag.)
KYP <sub>2</sub> Se <sub>6</sub>	<i>P</i> 2 <sub>1</sub> 2 <sub>1</sub>	6.7366(5)	7.4286(6)	21.603(2)		
KLaP <sub>2</sub> Se <sub>6</sub> <sup>a</sup>	<i>P</i> 2 <sub>1</sub> / <i>c</i>	12.425(1)	7.8047(5)	11.9279(9)	109.612(8)	
KCeP <sub>2</sub> Se <sub>6</sub>	<i>P</i> 2 <sub>1</sub> / <i>c</i>	12.396(2)	7.757(1)	11.872(2)	109.41(2)	2.43
KPrP <sub>2</sub> Se <sub>6</sub>	<i>P</i> 2 <sub>1</sub> / <i>c</i>	12.392(3)	7.735(1)	11.860(2)	109.28(2)	3.36
KGdP <sub>2</sub> Se <sub>6</sub>	<i>P</i> 2 <sub>1</sub> 2 <sub>1</sub>	6.759(1)	7.473(2)	21.596(4)		8.68

<sup>a</sup> First reported in ref 1.

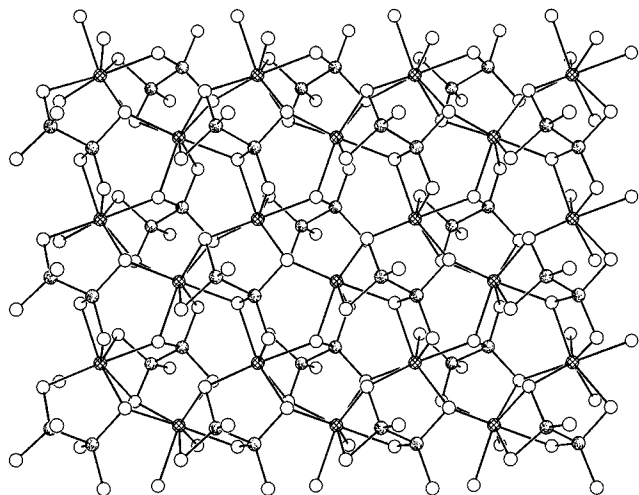


**Figure 2.** View of one layer of KYP<sub>2</sub>Se<sub>6</sub> down (001). Open circles are Se; dotted circles, P; crossed circles, Y; K atoms are not shown.

pointing out into the interlayer spacing. Each of the Se(6) atoms is coordinated to four potassium cations in a nearly square planar geometry with an average Se(6)–K distance of 3.579(4) Å and each potassium sits in an 8-fold coordinate site of selenium atoms. KGdP<sub>2</sub>Se<sub>6</sub> was found, by powder X-ray diffraction, to be isostructural with KYP<sub>2</sub>Se<sub>6</sub>; see Table 2. A list of the atomic coordinates and the important bond distances and angles can be found in Tables 3 and 4, respectively.

**Magnetism.** The magnetic susceptibility of each relevant compound in this study is listed in Table 2. All of the samples displayed a linear  $1/\chi$  dependence on temperature between 50 and 300 K, as shown in the typical Curie plot in Figure 4. The values in Table 2 are taken from the slope of the Curie plot of

**Table 3.** Fractional Atomic Coordinates and Equivalent Isotropic Displacement Parameters (Å<sup>2</sup> × 10<sup>3</sup>)<sup>a</sup> for KYP<sub>2</sub>Se<sub>6</sub>

	Wyckoff	<i>x</i>	<i>y</i>	<i>z</i>	<i>U</i> (eq)
K	4a	−0.6237(5)	0.4791(5)	−0.0044(2)	40(1)
Y	4a	0.2168(2)	0.6788(2)	0.25108(8)	11(1)
P(1)	4a	−0.1761(5)	0.4484(5)	0.1105(2)	10(1)
P(2)	4a	−0.3087(5)	0.6720(4)	0.1648(2)	12(1)
Se(1)	4a	0.0774(2)	0.3659(2)	0.16916(8)	13(1)
Se(2)	4a	−0.0670(2)	0.8726(2)	0.16815(8)	12(1)
Se(3)	4a	0.6311(2)	0.5498(2)	0.25662(8)	11(1)
Se(4)	4a	0.4113(2)	0.7627(2)	0.12731(8)	13(1)
Se(5)	4a	0.3916(2)	0.7339(2)	0.38084(8)	14(1)
Se(6)	4a	−0.1190(2)	0.5408(2)	0.01771(8)	21(1)

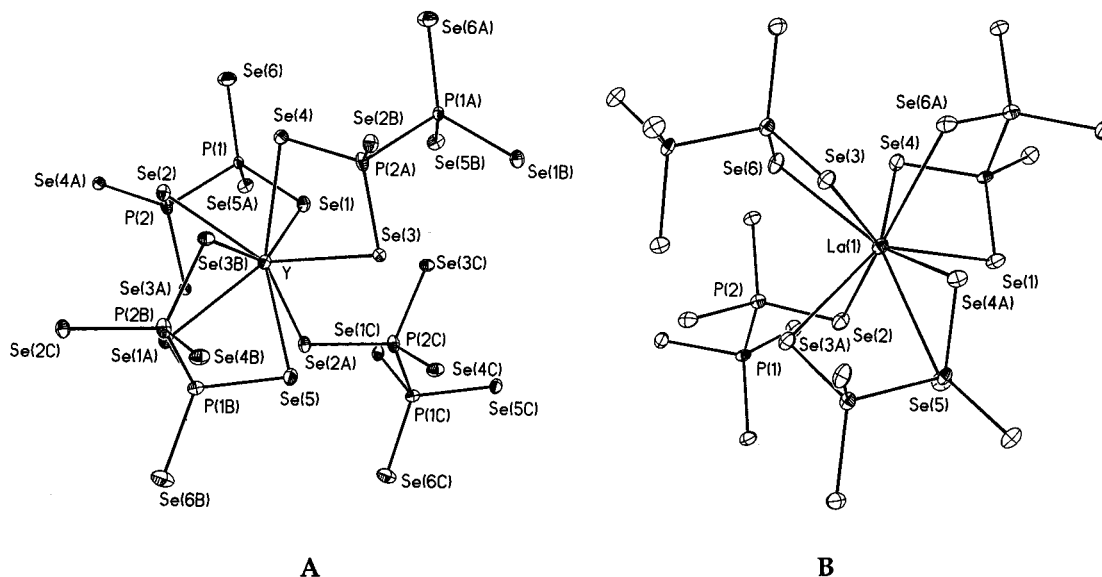
<sup>a</sup> *U*(eq) is defined as one-third the trace of the orthogonalized *U*<sub>*ij*</sub> tensor.

the paramagnetic data. The magnetic behavior of Ce, Pr, and Gd can be explained based on a simple set of unpaired f-electrons.

**Optical Properties.** The diffuse reflectance spectra of the compounds was examined. The observed, optical bandgaps of these materials all fall in the range 2.70–2.80 eV. There appears to be a low-energy transition that is found in every sample examined that could be related to impurities within the crystals or in the compounds themselves. A typical spectrum, plotted as log ( $\alpha/S$ ) vs energy, can be seen in Figure 5. No conductivity measurements were made as no suitable contacts to the insulating surfaces of the platelike crystals could be made.

## Discussion

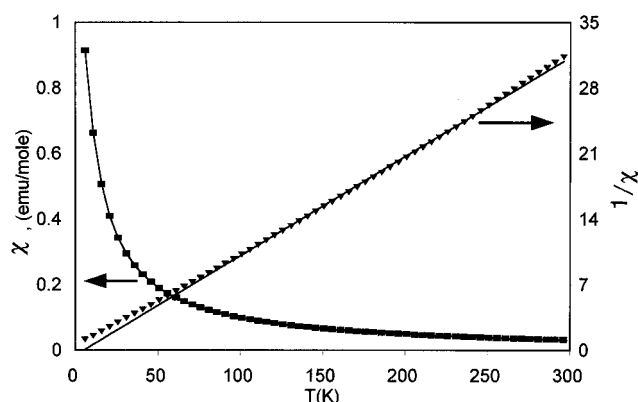
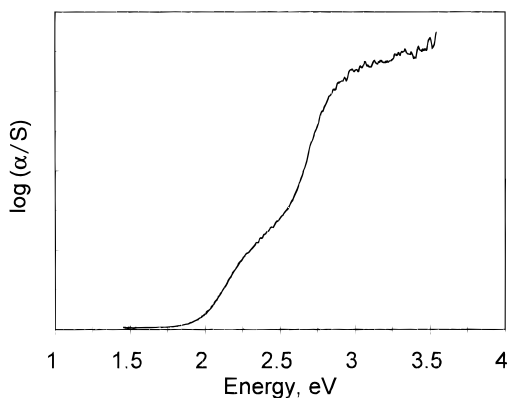
**KYP<sub>2</sub>Se<sub>6</sub>.** The structure of this more densely packed layered phase of selenodiphosphate(IV) anions may be attributed to the size differences between yttrium and the early lanthanides. The single-bond radii are 1.659 and 1.726 Å for yttrium and



**Figure 3.** Comparison of the environments around (A) yttrium in KYP<sub>2</sub>Se<sub>6</sub> and (B) lanthanum in KLaP<sub>2</sub>Se<sub>6</sub>.<sup>1</sup> The anisotropic (75%) thermal parameters are shown, and the labeling scheme pertains to the respective structure reports. Only one full coordination sphere around each rare-earth metal is shown.

**Table 4.** Pertinent Bond Distances (Å) and Angles (deg) for KYP<sub>2</sub>Se<sub>6</sub>

K–Se(6)	3.402(4)	K–Se(5)	3.450(4)
K–Se(6)	3.464(4)	K–Se(4)	3.549(4)
K–Se(6)	3.578(4)	K–Se(5)	3.590(4)
K–Se(2)	3.724(5)	K–Se(6)	3.873(4)
Y–Se(3)	2.945(2)	Y–Se(3)	2.954(2)
Y–Se(1)	2.971(2)	Y–Se(2)	2.989(2)
Y–Se(2)	3.039(2)	Y–Se(4)	3.042(2)
Y–Se(5)	3.068(2)	Y–Se(1)	3.068(2)
Y–Se(3)	2.945(2)	Y–Se(1)	2.971(2)
P(2)–Se(3)	2.218(4)	P(1)–P(2)	2.222(5)
P(1)–Se(5)	2.164(4)	P(2)–Se(2)	2.209(4)
P(1)–Se(1)	2.213(4)	P(1)–Se(6)	2.153(4)
P(2)–Se(4)	2.161(4)		
Se(3)–Y–Se(2)	74.81(5)	Se(3)–Y–Se(4)	66.96(5)
Se(1)–Y–Se(2)	72.29(5)	Se(3)–Y–Se(5)	69.11(5)
Se(3)–Y–Se(2)	92.72(5)	Se(3)–Y–Se(1)	93.82(5)
Se(2)–Y–Se(4)	69.52(5)	Se(2)–Y–Se(1)	79.84(5)
Se(6)–P(1)–Se(1)	118.9(2)	Se(6)–P(1)–Se(5)	115.8(2)
Se(6)–P(1)–P(2)	109.0(2)	Se(5)–P(1)–Se(1)	105.3(2)
Se(1)–P(1)–P(2)	102.4(2)	Se(5)–P(1)–P(2)	103.6(2)
Se(4)–P(2)–Se(3)	107.7(2)	Se(4)–P(2)–Se(2)	116.4(2)
Se(4)–P(2)–P(1)	112.7(2)	Se(2)–P(2)–Se(3)	112.5(2)
Se(3)–P(2)–P(1)	103.9(2)	Se(2)–P(2)–P(1)	103.0(2)

**Figure 4.** Plot of the magnetic susceptibility,  $\chi$  (emu/mole), left axis,  $1/\chi$ , right axis vs temperature (K) for KGdP<sub>2</sub>Se<sub>6</sub>. The line in the  $1/\chi$  plot represents the least-squares fit for a Curie plot.**Figure 5.** Diffuse reflectance spectrum,  $\log(\alpha/S)$  vs energy (eV), for KYP<sub>2</sub>Se<sub>6</sub>.

lanthanum, respectively.<sup>34</sup> The net result in these structures appears to be a smaller coordination sphere for yttrium (8-coordinate) than is observed for the lanthanum structure (9-coordinate). A comparison of the two coordination spheres is shown in Figure 3. Yttrium is coordinated in a “face-capping” arrangement by the Se(3B), Se(1A), and Se(5) atoms of one [P<sub>2</sub>Se<sub>6</sub>]<sup>4-</sup> unit, and has edge-sharing arrangements from two other [P<sub>2</sub>Se<sub>6</sub>]<sup>4-</sup> units, and finally a single, P–Se–Y end-on

coordination from a fourth [P<sub>2</sub>Se<sub>6</sub>]<sup>4-</sup> anion, similar to the bonding seen in Ag<sub>4</sub>P<sub>2</sub>Se<sub>6</sub>.<sup>5</sup> In the 9-coordinate lanthanum case, there are two “face-capping” [P<sub>2</sub>Se<sub>6</sub>]<sup>4-</sup> anions per La.

Other structural features are also prominent. Unlike KLaP<sub>2</sub>Se<sub>6</sub>, the yttrium phase has only single, rectangular layers of yttrium atoms linked by the phosphate groups. The phosphate anions are located on the edges of the layers with one selenium atom pointing into the interlayer gap, coordinated only to P(1) and interacting with the interlayer potassium cations. This arrangement, compared schematically in **1** in Chart 1, is more like the oxo-phosphate organization in H<sub>2</sub>Zr(PO<sub>4</sub>)<sub>2</sub><sup>35</sup> than the selenophosphate organization in KLaP<sub>2</sub>Se<sub>6</sub> or in any other layered MPQ<sub>n</sub> structure type we have seen.<sup>4</sup>

**Structural Relationships.** The discovery of relationships between structures often relies on comparisons of unit cell volumes, symmetries, or Pearson symbols.<sup>36</sup> Many relationships are obscured in symmetry (or the lack thereof), and more rigorous, *ab initio* methods are required to unveil those structural relationships. We have compared the Parthé anionic tetrahedral partial structure components of the two polytypic rare-earth-metal selenodiphosphate structures with other chalcophosphate compounds in an attempt to fully characterize and understand our new structures.<sup>24,37–39</sup>

According to the Parthé valence electron concentration (VEC) electron counting rules, the [P<sub>2</sub>Se<sub>6</sub>]<sup>4-</sup> anion in our compounds can be expressed by a numerical classification code that defines the bonding within and between polyanionic tetrahedral units. The Parthé VEC electron counting scheme for tetrahedral complexes, based on the 8 - N electron rules for C(x)<sub>m</sub>C'<sub>m</sub>A<sub>n</sub>, can be summarized as follows: Polycationic valence compounds are compounds that possess >8 electrons per A anion in [C'<sub>m</sub>A<sub>n</sub>]<sup>(mx)-</sup>, polyanionic valence compounds have < 8 electrons per A anion, and valence precise compounds have exactly 8 electrons per A anion, where the valence electron concentration per anion is VEC<sub>A</sub>. This value can be derived by counting the number of valence electrons donated by the anions, A (in our case, Se), the cations, C (i.e. K, La), and the tetrahedral heteroatom, C' (P), and dividing by the number of anions, n. In our case, C is K + La or K + Y, yielding a VEC<sub>A</sub> = 8.3333. This value, being greater than 8.0, indicates that this is a polycationic complex ion and there should be a central atom bond, C'C' = 1.0, between the two P (IV) atoms of the [P<sub>2</sub>Se<sub>6</sub>]<sup>4-</sup> unit. Since there are no corner-sharing or edge-sharing tetrahedra in the structure, C'AC' is 0.0. From this, we arrive at a classification code for the [P<sub>2</sub>Se<sub>6</sub>]<sup>4-</sup> anion in our K(RE)P<sub>2</sub>Se<sub>6</sub> phases, shown schematically in **2**, of

$${}^{C'}\text{VEC}_A/C'AC' = {}^{1.0}8.3333/0 \quad (2)$$

which we use for the comparison of our anionic substructure to other anionic substructures. Structure **2** shows the [P<sub>2</sub>Se<sub>6</sub>]<sup>4-</sup>

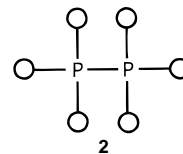
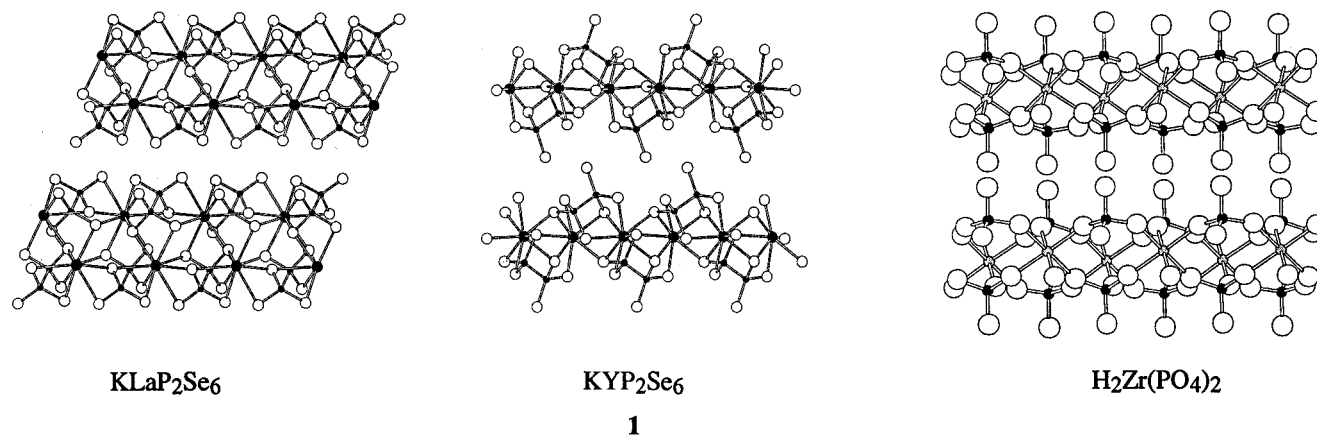
(35) Troup, J. M.; Clearfield, A. *Inorg. Chem.* **1977**, *16*, 3311(36) Pearson, W. B. *The Crystal Chemistry and Physics of Metals and Alloys*; Wiley-Interscience: New York, 1972.(37) Parthé, E. *Elements of Inorganic Structural Chemistry*; K. Sutter Parthé: Lancy, Switzerland, 1990; p 100.(38) Parthé, E.; Chabot, B. *Acta Crystallogr.*, **B 1990**, *46*, 7.(39) Parthé, E. In *Modern Perspectives in Inorganic Crystal Chemistry*, NATO ASI Series 382; E. Parthé, Ed.; Kluwer: Dordrecht, NL, The Netherlands, 1992; Vol. 382.(34) Pauling, L.; Kamb, B. *Proc. Natl. Acad. Sci. U.S.A.* **1986**, *83*, 3569.

Chart 1



unit with open circles representing “non-interacting” selenium atoms; the lack of any C'AC' bonds indicates a lack of complex connectivity between the  $[P_2Se_6]^{4-}$  anions in the structure; that is, there are no corner-sharing or edge-sharing interactions between  $[P_2Se_6]^{4-}$  anions. This scheme also accounts for the P–P bond in the complex anionic unit.

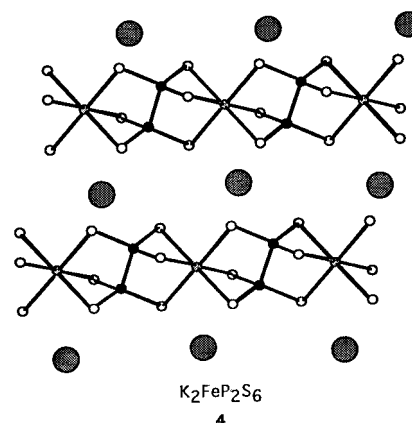
The Parthé VEC rules do not, however, distinguish the different connectivity environments for the different lanthanides (Y, Gd and La, Ce, Pr) in the two different structures. Nevertheless, we can use the index to select several comparative isoelectronic structures that possess the same phosphate building blocks. The structures we have chosen for comparison are  $Ag_4P_2S_6$ ,  $K_2FeP_2S_6$ , and the  $MPS_3$  structure types.<sup>4–7</sup> It should be noted that Kanatzidis and co-workers have prepared a bismuth-based selenodiphosphate-layered compound that is related to the  $KLaP_2Se_6$  type;<sup>15</sup> however, the bonding to the bismuth sites and the lanthanum sites are different in coordination number, as one would expect. The similarities between these structures has been addressed,<sup>1</sup> but the same Parthé VEC relationships apply for the bismuth phase as they do for our rare-earth-metal phases, assuming one treats bismuth as a 3-electron donor and not in a strict Zintl fashion. Finally, on the basis of the VEC method of classification, it is also clear that our structures will not have many structural similarities to compounds such as  $Ag_4P_2S_7$ ,  $Hg_2P_2S_7$ , or  $A_4Ti_2P_6Q_{25}$  which contain corner-sharing tetrahedral units such as  $[P_2Q_7]^{4-}$ , with classification codes of <sup>0.08.000/1.0.</sup><sup>19,23,40,41</sup>

**$Ag_4P_2S_6$ .** A simple VEC calculation shows that this compound and our title compounds are isoelectronic,  $M'_4P_2Q_6$ . Using eq 2 above, one can calculate a classification code for the  $[P_2S_6]^{4-}$  unit in  $Ag_4P_2S_6$  as <sup>1.08.333/0.</sup><sup>5</sup> Given the similarities in charge and classification code, there should be some recognizable pieces of the  $Ag_4P_2S_6$  structure in our structures, and vice versa.

In this structure, there are six crystallographically unique silver atoms that are in tetrahedral or trigonal pyramidal environments of sulfur. The coordination of the thiodiphosphate groups to the silver atoms shows features similar to our  $K(RE)P_2Se_6$  polytypes; bonding is either through terminal interactions (corners of the Ag tetrahedra) or through edge bridging, as seen in the relationship Se(4)–Y–Se(3), in Figure 3. More importantly, this structure, like  $KYP_2Se_6$ , is composed of single-layers of thiodiphosphate. These layers are joined together by silver atoms, creating a three-dimensional structure. However, upon substitution of one-fourth of the appropriate silver atoms by

potassium ions, we do not arrive at a similar structure. A schematic comparison of the layers of the two structure types is shown in structure 3 in Chart 2.

**$K_2FeP_2S_6$ .** This structure, also being isoelectronic with our  $K(RE)P_2Se_6$  polytypes, possesses the  $[P_2S_6]^{4-}$  building block with <sup>1.08.333/0</sup> for a classification code.<sup>6</sup> This structure crystallizes in a monoclinic space group with chains of face-sharing sulfur octahedra running along (100). The centers of the octahedra of the chains are alternately filled with iron or P–P dimers. The net result is isolated columns of octahedra separated from each other by potassium cations, shown in 4.



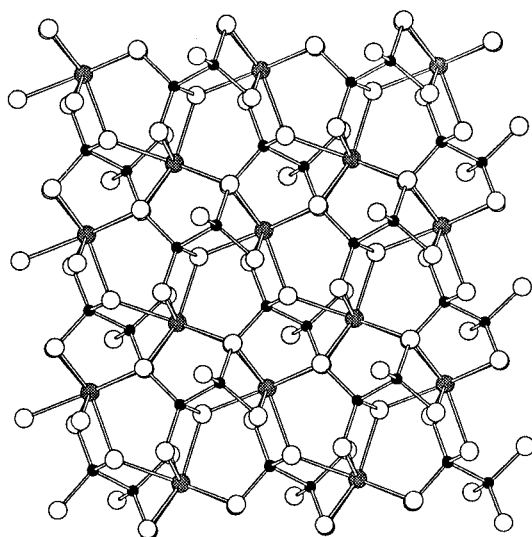
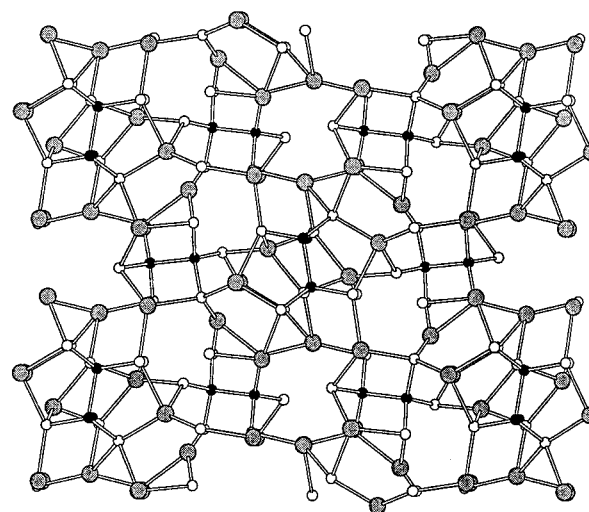
The  $K_2FeP_2S_6$  structure could be considered to be a reduced form of  $FePS_3$ , see below, as the coordination environments of the phosphorous and iron atoms are nearly identical, except for the fact that the slabs of  $FePS_3$  have been sliced into ribbons by the introduction of two more electrons into the system from potassium. Brockner and co-workers refer to this 1-dimensional compound as a “densest packing of rods” in the cell, whereas  $FePS_3$  results from a densest packing of atoms in sheets.

Although  $K_2FeP_2S_6$  and our  $K(RE)P_2Se_6$  polytypes are isoelectronic and contain the same building blocks, we could not find an easy link between the structures. We treated this structure as we did for  $Ag_4P_2S_6$  above; a simple replacement of one atom for another does not lend itself to a simple relationship between our structures and  $K_2FeP_2S_6$ . However, we might imagine removing one layer of “interchain” potassium ions (giving  $K_{(2-1)}MP_2S_6$ , where M must be a trivalent lanthanide, RE) and compressing the chains together through S–RE–S interactions in an expanded coordination sphere for RE, 5. In so doing, the double layered  $KLaP_2Se_6$  type begins to emerge (see 1 above for comparison). We need to imagine that the chains will “buckle” to accommodate the 9-fold

(40) Toffoli, P.; Khodadad, P.; Rodier, N. *Acta Crystallogr., B* **1977**, *33*, 1492.

(41) Tremel, W. Manuscript in preparation.

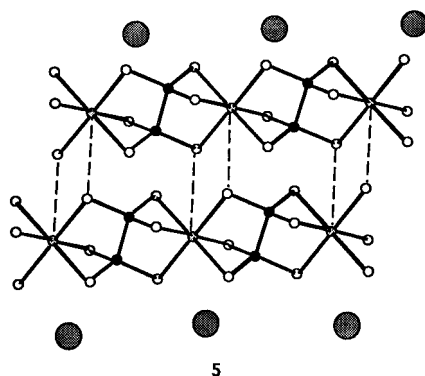
Chart 2

KYP<sub>2</sub>Se<sub>6</sub>Ag<sub>4</sub>P<sub>2</sub>S<sub>6</sub>

3

coordination requirement of the lanthanum, hence resulting in the formation of the porous layered structure.

Schematically, this structure can be viewed in 6. In this structure, the transition metal atoms are found in octahedral holes

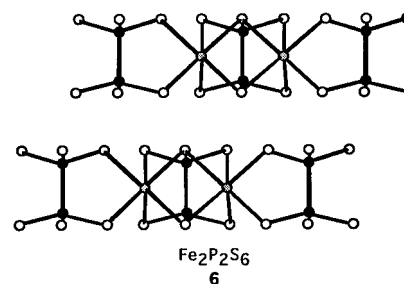


5

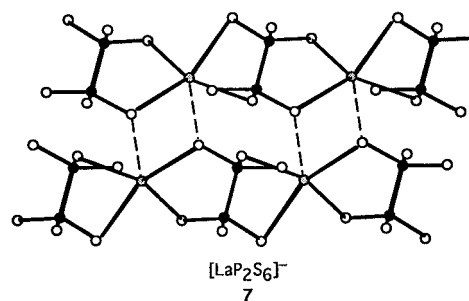
Alternatively, if the chains are condensed in a fashion so as to yield a single layer structure, less bucking is required of the rods and the KYP<sub>2</sub>Se<sub>6</sub> type emerges. Although the relationships between these structures are not so obvious, careful manipulation of the K<sub>2</sub>FeP<sub>2</sub>S<sub>6</sub> structure yields structures that, with the right pair of "spectacles",<sup>42</sup> can be viewed as relatives of our K(RE)-P<sub>2</sub>Se<sub>6</sub> family of compounds.

**MPQ<sub>3</sub>.** A comparison of our structures to the isoelectronic M<sup>II</sup>PS<sub>3</sub> type was also in order given that the Parthé index of the [P<sub>2</sub>Se<sub>6</sub>]<sup>4-</sup> anion in this phase matches that found in our two phases. A comparison of KLaP<sub>2</sub>Se<sub>6</sub> and KYP<sub>2</sub>Se<sub>6</sub> can be made by closely examining the packing of the lanthanide atoms and the selenodiphosphate (IV) groups. First, we shall turn our attention to KLaP<sub>2</sub>Se<sub>6</sub>.

The M<sup>II</sup>PS<sub>3</sub> hexagonal structure type consists of a hexagonal-closest packed formation of sulfur.<sup>4</sup> In this structure, the [P<sub>2</sub>S<sub>6</sub>]<sup>4-</sup> units fill one-sixth of the octahedral holes. Another one-third of the octahedral holes are filled with the divalent transition metal cation. This leaves exactly half of the octahedral holes empty. These are arranged in such a way as to create a layered structure with a van der Waals gap between layers of [M<sub>2</sub>P<sub>2</sub>S<sub>6</sub>].

Fe<sub>2</sub>P<sub>2</sub>S<sub>6</sub>  
6

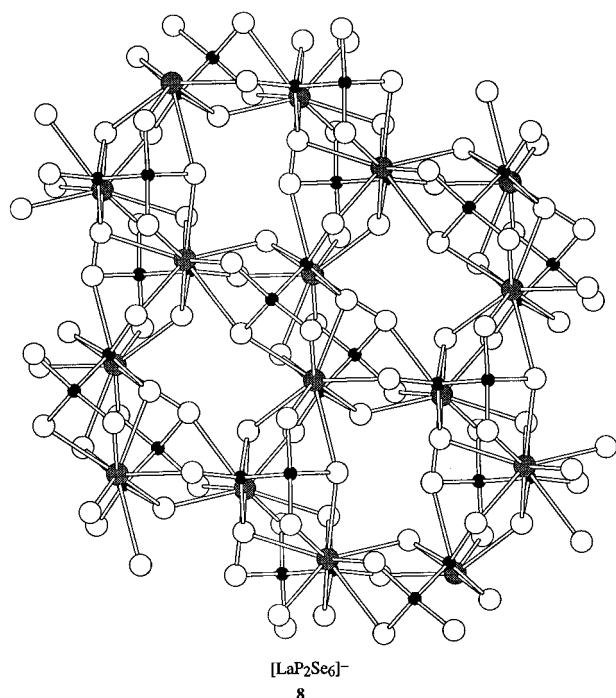
in the structure with each [P<sub>2</sub>Q<sub>6</sub>]<sup>4-</sup> unit capping a trigonal face of 6 octahedra. In the case of lanthanum, a 6-fold coordination sphere is insufficient, primarily due to the sizes of the lanthanide. The lattice must reorganize in order to accommodate a higher coordinating metal ion. This can be easily accomplished in the case of KLaP<sub>2</sub>Se<sub>6</sub> by moving the phosphates to the outer edges of the layers of an [M<sub>2</sub>P<sub>2</sub>Q<sub>6</sub>] layer and allowing two layers to condense together, as shown in 7. When this occurs, the

[LaP<sub>2</sub>Se<sub>6</sub>]<sup>-</sup>  
7

selenium atoms from one selenodiphosphate (IV) can bridge to the next layer and fuse the bilayer structure, indicated by the dashed lines.

One question that is raised is how does the structure account for the "loss" of the octahedral holes in the [M<sub>2</sub>P<sub>2</sub>Q<sub>6</sub>] interlayer spacing? Since only half of the interlayer "holes" are apparently lost by condensing every other layer (the other half remain empty, the interlayer spacing) we need only account for one-

fourth of the holes in the lattice. Looking down on the layers in  $\text{KLaP}_2\text{Se}_6$ , one finds a set of twisted "triangular" arrangements of the lanthanides, offset by an angle of  $\sim 50^\circ$ . A view down (010) of the  $\text{KLaP}_2\text{Se}_6$  layers is shown in **8**. The holes in the



layers correspond to one of the metal array sites in the  $[\text{Fe}_2\text{P}_2\text{Q}_6]$  parent. These holes create a layer that has the formula  $[\text{M}_2^{\text{III}}\text{P}_4\text{Se}_{12}]^{2-}$ . Overall, then, this arrangement possesses two empty "holes": a hole in the double layer and the remaining holes in the interlayer spacing. The "holes" in the layers of this structure are then filled with the counteranion,  $\text{K}^+$ , that acts as the ionic "glue" holding the layers together, leaving the interlayer gap unfilled.

Finally, closely examining the  $\text{KYP}_2\text{Se}_6$  type, we find that the single layer is quite like the single layered structure of  $\text{MPS}_3$ . Again, we may account for the charges by doubling the unique unit to give  $\text{M}^{\text{II}}_2\text{P}_2\text{S}_6$ . If half of the  $\text{M}(\text{II})$  atoms are replaced with  $\text{Y}(\text{III})$  and the other half with  $\text{K}^+$ , the electron counting is balanced.

The network of yttrium atoms in the structure is square, Figure 2, instead of hexagonal, as in  $\text{MPS}_3$ . Although this square packing of yttrium atoms is less efficient than the hexagonal packing of  $\text{M}(\text{II})$  in  $\text{MPS}_3$ , the increased coordination number of yttrium over  $\text{M}(\text{II})$  leaves no room in the layers for the potassium cations. As a consequence, the potassium cations must assemble between the layers, near  $\text{Se}(6)$ , to balance the charge of the negative layers, much like the way cations assemble in  $\text{A}_2\text{Zr}(\text{PO}_4)_2$  (see **1** above).

**Magnetic Susceptibility Measurements.** A plot of  $\chi$  (molar susceptibility) and  $1/\chi$  vs temperature is shown in Figure 4 for  $\text{KGdP}_2\text{Se}_6$ . Plots of the La polytype with Ce and Pr are similar in nature. The  $1/\chi$  vs temperature data was subjected to a linear regression analysis that yields the susceptibility values given

in Table 2. Within experimental error and after applying the diamagnetic core corrections, these values are consistent with the expected unpaired f-electrons found for trivalent rare-earth-metal compounds. The exception being  $\text{KGdP}_2\text{Se}_6$ , which displays a susceptibility slightly larger than expected. This may be due in part to a small percentage of impurity in the sample which would lower the mass (and hence increase the apparent molar susceptibility).

**Diffuse Reflectance Measurements.** The diffuse reflectance spectra for all of the compounds studied reveal that these compounds are broad bandgap materials with a gap between 2.7 and 2.8 eV. There also appears to be a small absorption at lower energies that may be related to some impurities in the crystals chosen for examination. These impurities may originate from glassy particulates of the melt trapped within the crystals as they form. In fact, close inspection of several pale yellow crystals does reveal small, dark impurities within the crystals. Since these particles are trapped within the crystals, there does not appear to be any means by which they may be washed out of the solids.

A typical diffuse reflectance spectrum is shown in Figure 5. The spectrum is plotted as  $\log(\alpha/S)$  vs energy, where  $\alpha$  is the absorption coefficient and  $S$  is the scattering factor of the solid. Conversion of reflectance data to  $(\alpha/S)$  can be achieved by the Kubelka–Munk relationship and has been discussed elsewhere.<sup>33,43</sup>

## Conclusions

Two polytypes of the general formula  $\text{K}(\text{RE})\text{P}_2\text{Se}_6$  have been examined structurally and physically. The two structures were described by a valence electron concentration analysis and compared to three other potentially related structure types:  $\text{Ag}_4\text{P}_2\text{S}_6$ ,  $\text{K}_2\text{FeP}_2\text{S}_6$ , and  $\text{FePS}_3$ . Although our two polytypic structures could be related, in part, to these structures, they represent a unique family of layered solids based on rare-earth-metal elements. Magnetic data suggest that the rare-earth metals are magnetically isolated in the structure and communicate only in a Curie paramagnetic fashion. Diffuse reflectance spectroscopy (and the poor conductive nature of these) suggests the title compounds are broad band gap materials. We are currently examining the high pressure behavior of these polytypes.<sup>44</sup>

**Acknowledgment.** P.K.D. would like to acknowledge financial support from the Research Corporation, Cottrell Fellowship, and Colorado State University. Ames Laboratory is operated for the U.S. Department of Energy by Iowa State University under Contract No. W-7405-ENG-82. We also thank Susie Miller and Casey Raymond for crystallographic assistance and Catherine Zelenski for EDS.

**Supporting Information Available:** A table of formulas for calculating classification codes (1 page). One X-ray crystallographic file, in CIF format, is available for  $\text{KYP}_2\text{Se}_6$ . Access and/or ordering information is given on any current masthead page.

IC9516121

(43) McCarthy, T. J.; Tanzer, T. A.; Kanatzidis, M. G. *J. Am. Chem. Soc.* **1995**, *117*, 1294.

(44) Lorenz, B.; Orgzall, I.; Raymond, C. C.; Dorhout, P. K.; Hochheimer, H. D. Manuscript in preparation.